

Aromatic/perfluoroaromatic self-assembly effect: an effective strategy to improve the NLO effect†

Wenbo Wu,^a Qi Huang,^a Guofu Qiu,^b Cheng Ye,^c Jingui Qin^a and Zhen Li^{*a}

Received 16th May 2012, Accepted 12th July 2012

DOI: 10.1039/c2jm33129b

In this paper, a facile route was designed to prepare four new second-order nonlinear optical (NLO) polyaryleneethynylenes containing normal aromatic or perfluoroaromatic rings as isolation groups *via* a simple Sonogashira coupling reaction. For comparison, their small molecule models were also synthesized to investigate the aromatic/perfluoroaromatic (Ar–Ar^F) self-assembly effect existing between the isolation groups and polymer main chain. Thanks to the presence of the self-assembly effect, the NLO effect and stability of these polymers were enhanced in a large degree. The NLO coefficient of **P4** reached up to 166.7 pm V⁻¹, which is, to the best of our knowledge, the new record reported so far for linear polymers using simple azobenzenes as the chromophore moieties.

Introduction

There are various noncovalent intermolecular interactions that can be used for the construction of supramolecular self-assemblies in molecular glasses, such as electrostatic interactions between charges, multiple hydrogen bonds, metal–organic ligand coordination, π – π aromatic interactions, van der Waals interactions and so on.¹ Among them, noncovalent interactions between aromatic groups have been widely used in organic and polymeric opto-electronic materials.² Although a considerable amount of work concerning the stacking of aromatic rings has concentrated on phenyl–phenyl interactions, there is a growing interest in the interactions of phenyl and perfluorophenyl groups. Patrick and Prosser^{3a} first recognized that a 1 : 1 mixture of benzene (with a melting point of 5.5 °C) and hexafluorobenzene (with a melting point of 4 °C) could form a complex, which melts at 24 °C, much higher than 5.5 or 4 °C. Although pure benzene adopts an edge-to-face structure in the solid-state, it has been determined that the structure of the benzene/hexafluorobenzene mixture consists of alternating stacks of these two molecules, due to the electropositive activity of hexafluorobenzene (Chart 1).^{2c,3}

In the field of opto-electronic materials science, most of the second-order nonlinear optical (NLO) materials have been developed for applications in photonic devices, such as

high-speed electro-optic modulators, optical switches, frequency converters and so on.⁴ One major obstacle that is hindering the rapid development of this field is the relatively low macroscopic NLO activities, in comparison with large $\mu\beta$ values of the organic chromophores, because of the strong dipole–dipole interactions among the chromophore moieties with the donor– π –acceptor structure in the polymeric system. This interaction results in the poling-induced noncentrosymmetric alignment of chromophore moieties (necessary for the materials to exhibit the macroscopic NLO effect), a daunting task during the poling process under an electric field.⁵ Recently the aromatic/perfluoroaromatic (Ar–Ar^F) self-assembly effect was first used in nonlinear optical (NLO) materials by Jen and co-workers in 2007.⁶ By utilizing aromatic/perfluoroaromatic dendron-substituted NLO chromophores through the presence of these complementary Ar–Ar^F interactions, they developed a new class of molecular glasses (Charts S1

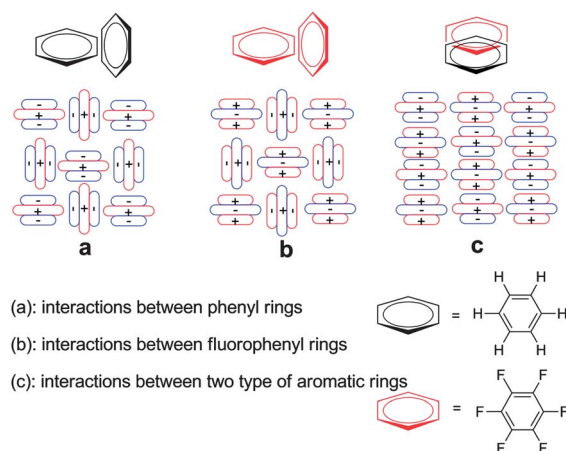


Chart 1 Different interactions between different aromatic rings.

^aDepartment of Chemistry, Wuhan University, Wuhan 430072, China. E-mail: lizhen@whu.edu.cn; lichemlab@163.com; Fax: +86 027 68755363

^bCollege of Pharmacy, Wuhan University, Wuhan 430072, China

^cInstitute of Chemistry, The Chinese Academy of Sciences, Beijing 100080, China

† Electronic supplementary information (ESI) available: Structure of some dendritic NLO chromophores containing perfluoroaromatic rings, and some polymers containing isolation groups. The IR spectra, NMR spectra, UV-vis spectra, TGA thermograms of polymers **P1–P4** and their model molecules. See DOI: 10.1039/c2jm33129b

and S2†), which exhibited improved poling efficiency and greatly enhanced macroscopic NLO effects.⁶ However, so far, there have been no other successful cases reported. Thus, further research is still needed to check the above mentioned exciting increase of the macroscopic NLO effect derived from the Ar–Ar^F self-assembly effect and understand this abnormal phenomenon in more depth.

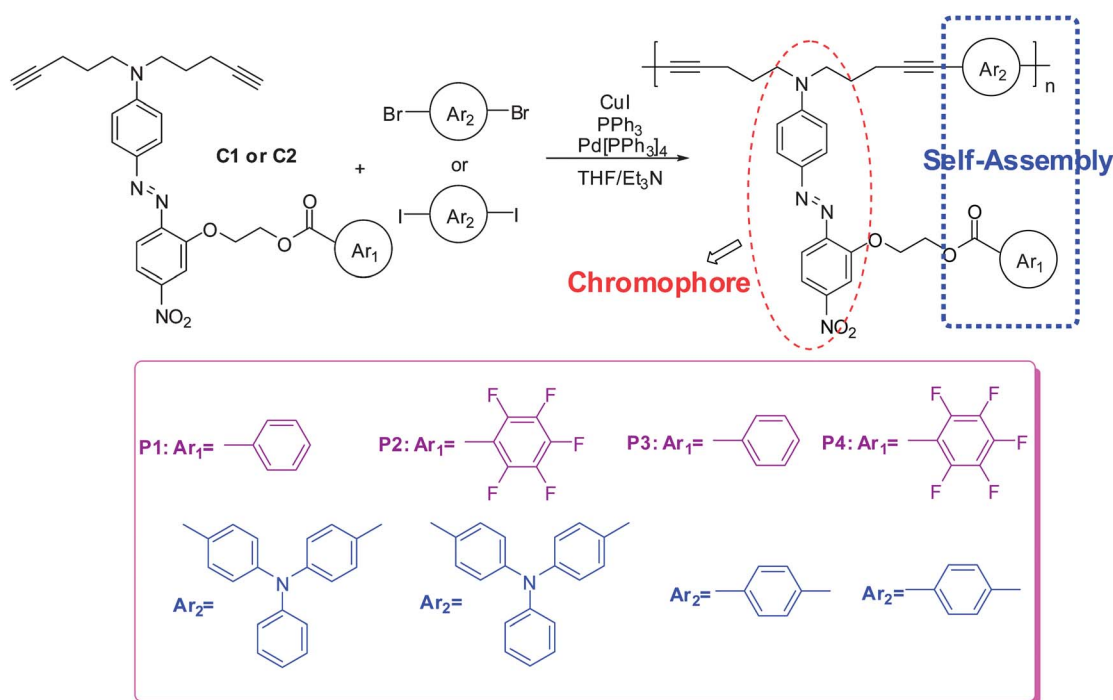
From 2006, we have systematically designed many different types of NLO dendronized polymers containing different isolation groups with different sizes in the chromophore moieties (Charts S3–S8†). Based on the obtained experimental results, we proposed the concept of a “suitable isolation group”, for the enhancement of the macroscopic NLO effect of polymers.⁷ Considering the above mentioned aromatic/perfluoroaromatic (Ar–Ar^F) self-assembly effect, we were wondering if this effect could be coupled with the concept of a “suitable isolation group”, to further improve the NLO performance of the resultant polymers. From this standpoint, four new simple NLO polyaryleneethynylenes **P1–P4** (Scheme 1) containing nitro-based azobenzene as the chromophore were designed and prepared successfully *via* the Sonogashira coupling reaction. In **P2** and **P4**, the isolation groups were perfluoroaromatic rings instead of the normal phenyl rings in **P1** and **P3**. This change could only alter the loading density of the effective chromophore moieties to a very limited degree, which would facilitate the comparison of their properties on the same level. To aid the investigation of the Ar–Ar^F self-assembly effect conveniently, six small model molecules **M1–M6** were also synthesized. Analyzing the properties of **P1** and **P3** containing normal phenyl rings as the isolation groups, its corresponding chromophore **C2** and model molecules, there was much evidence such as different NMR and IR spectra, to confirm the presence of the self-assembly in **P2** and **P4**. Excitingly, these interactions resulted in much higher NLO coefficients, with the d_{33} value of **P4** reaching

up to 166.7 pm V⁻¹, which is the highest value so far reported for linear polymers using simple azobenzenes as the chromophore moieties, to the best of our knowledge. Herein, we would like to present the syntheses, characterization and properties of these NLO polymers in detail.

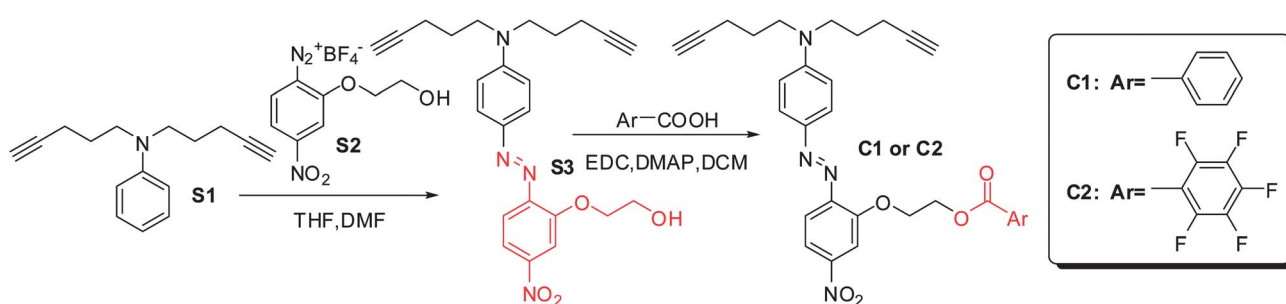
Result and discussion

Synthesis

The overall pathway of the monomer synthesis is presented in Scheme 2. Usually, in the azo-coupling reaction, diazonium hydrochloride was used as the azo reagent, due to its high reaction activity.⁸ However, for the synthesis of chromophore **S3**, there was nearly no product yielded using this route, even when we changed the reaction conditions including, the concentration and pH values. Thus, fluoborate salt was used instead of the normal hydrochloride salt as the azo reagent.⁹ Then, the monomers (chromophores **C1** and **C2**) were prepared by the esterification of chromophore **S3** with benzoic acid or pentafluorobenzoic acid under mild conditions, in which the phenyl or pentafluorophenyl groups act as isolation spacers. Finally, the target NLO polymers **P1–P4** could be prepared successfully *via* a typical Sonogashira cross-coupling reaction between different chromophores and aryl halides, catalyzed by Pd(PPh₃)₄, PPh₃, and CuI, similar to our previous work,^{8a} as shown in Scheme 1. The reactivity of different aryl halides was very different during the Sonogashira cross-coupling procedure: aryl iodide could react with terminal alkyne below room temperature, while aryl bromide only reacts at higher temperatures such as 50–60 °C. However, to ensure there were no other unnecessary groups to affect the self-assembly effect, *N,N*-bis-(4-bromophenyl)benzenamine was still used as the comonomer



Scheme 1 The synthesis of NLO polymers **P1–P4**.



Scheme 2 The synthesis of monomers **C1** and **C2**.

(since the synthesis of *N,N*-bis(4-iodophenyl)benzenamine was very difficult), although the aryl bromide had a lower reactivity. Anyhow, the total route to the synthesis of the target polyaryleneethynyls **P1–P4** was very simple, making it convenient to make a comparison of their tested NLO properties.

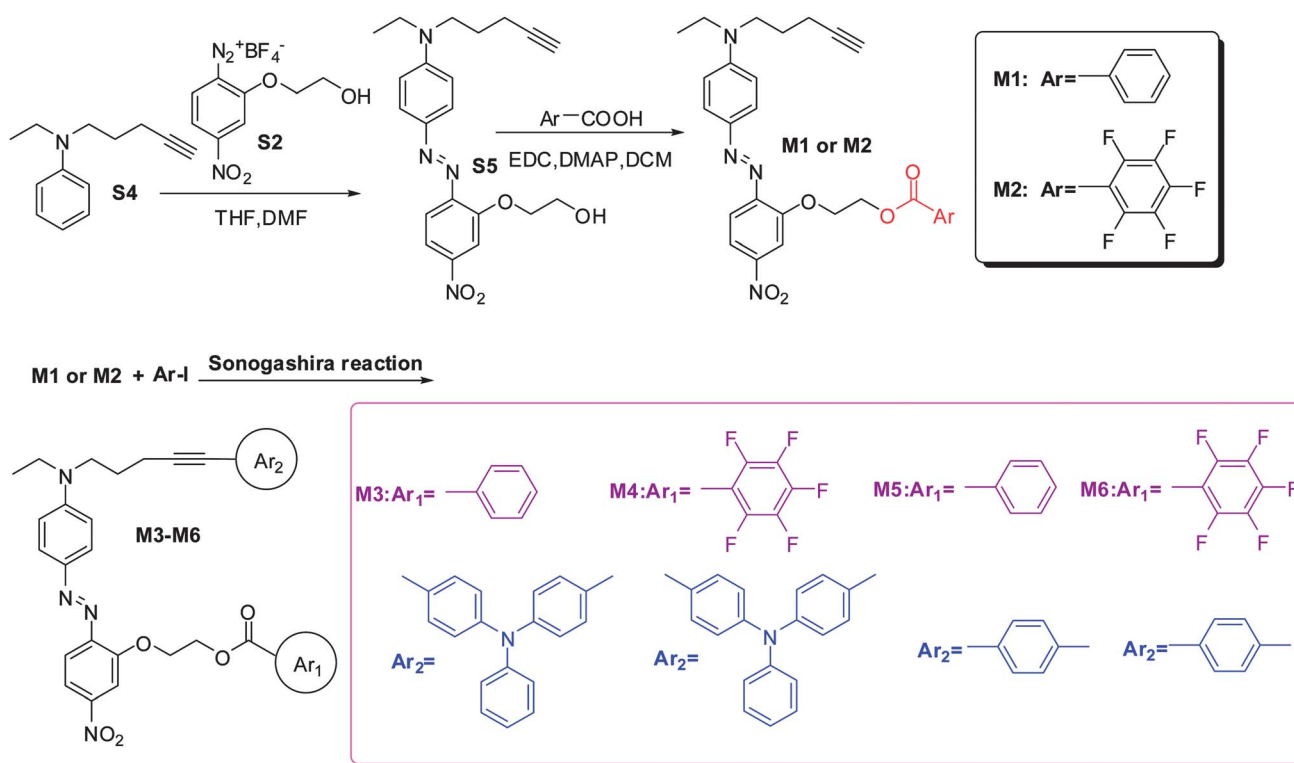
The synthesis of the model molecules **M1–M6** was similar to the monomers **C1–C2** and the NLO polymers **P1–P4**, and the specific synthetic route is shown in Scheme 3: the azo based chromophore **S5** was prepared *via* the azo-coupling reaction using fluoborate salt **S2** as the azo reagent; and then, **M1** and **M2** were prepared by esterifications; at last, **M3–M6** were also obtained *via* the Sonogashira cross-coupling reaction.

Characterization and self-assembly effect

The prepared chromophores and polymers were characterized by spectroscopic methods, and all gave satisfactory spectral data (see experimental section and ESI† for detail data). Fig. S1†

showed the FT-IR spectra of the polymers **P1–P4**, in which the absorption bands associated with the nitro groups and carbonyl groups were at about 1338, 1517 cm^{-1} and 1720 cm^{-1} or 1740 cm^{-1} respectively, showing that the chromophore and isolation groups were stable during the Sonogashira polymerization reactions. Different activities of phenyl groups or pentafluorophenyl groups led to different wavenumbers of the carbonyl group. At the same time, an absorption band derived from the $\equiv\text{C-H}$ stretching vibrations disappeared at about 3277 cm^{-1} in the FT-IR spectra of polymers **P1–P4**, indicating that the polymerizations were successful.

NMR spectroscopy is an especially useful tool to illustrate the successful synthesis of products in organic chemistry. Fig. 1 shows the ^1H NMR spectra of **S3**, **C2** and **P2**, as well as their chemical structures, as an example to show the successful synthesis, while the original spectra of the other compounds are listed in Fig. S2–S28 in the ESI.† In the spectrum of chromophore **S3**, no unexpected resonance peaks were observed, and the chemical shifts



Scheme 3 The synthesis of model molecules **M1–M6**.

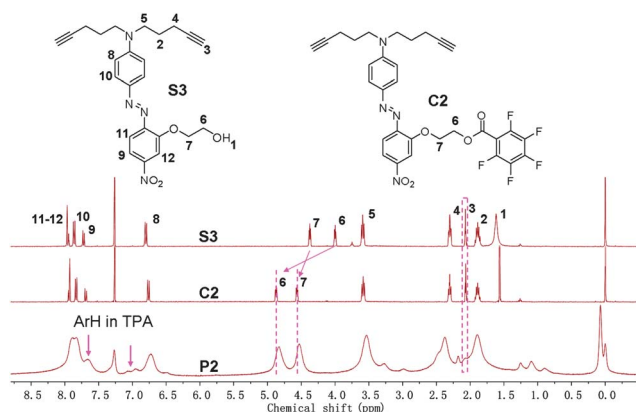


Fig. 1 ^1H NMR spectra of S3, C2 and NLO polymer P2 in chloroform-*d*.

were consistent with the proposed structure (the corresponding peaks are marked in Fig. 1). After esterification by pentafluorobenzoic acid, the $-\text{OH}$ peak (marked 1) disappeared, while the chemical shifts of the $-\text{COOCH}_2-$ group (marked 6) and $-\text{OCH}_2-$ (marked 7) became larger, due to the electron withdrawing activity of the pentafluorobenzoic groups. After polymerization, all the peaks of P2 showed an apparent inclination of signal broadening, and the disappearance of the single peaks associated with the protons of $\text{C}\equiv\text{CH}$ (marked 3) around 2.05 ppm, and some ArH from the comonomer appeared, confirming that the polymerization was successful. The structure of the other polymers could be also confirmed in a similar way. There was an interesting phenomenon observed in the ^1H NMR spectra. Except the peaks assigned to the protons of the isolation groups (phenyl or pentafluorophenyl), there was another difference between the ^1H NMR spectra of C1 and C2: the chemical shift of the $-\text{COOCH}_2-$ group in C1 was 4.80 ppm, but 4.88 ppm in C2. This should be ascribed to the different electron behavior of the phenyl and pentafluorophenyl groups. Due to the high electronegativity of fluorine atom, the perfluoroaromatic rings were electropositive, making the electron withdrawing activity of the pentafluorobenzoic groups much stronger than that of the benzoic ones. Thus, the chemical shifts of protons next to them were different. After polymerization, the chemical shifts of protons next to the pentafluorobenzoic ($-\text{COOCH}_2-$) in the ^1H NMR spectra of P2 and P4 became smaller, in comparison with its corresponding chromophore C2 (Fig. 1 and 2A), disclosing that the electron withdrawing activity of pentafluorobenzoic groups became weaker, and the electron density distribution on the perfluoroaromatic rings became higher. This phenomenon could be caused by the self-assembly effect between the perfluoroaromatic rings and the aromatic ones in the comonomer units. Furthermore, the change of this peak in P2 was larger than that in P4, indicating that the self-assembly effect in P2 was stronger than P4, possibly due to its larger comonomer triphenylamine (TPA) unit. To further prove this point, the ^1H NMR spectra of the model molecules were also tested. As expected, the chemical shifts of protons next to the benzoic group ($-\text{COOCH}_2-$) in M1, M3 and M6 were the same. However, differences occur in the model molecules bearing pentafluorophenyl groups. The chemical shift of the $-\text{COOCH}_2-$ group in M2 was 4.88 ppm, the same as in C2. Just after the Sonogashira reaction, it changed to 4.85 or 4.87 in

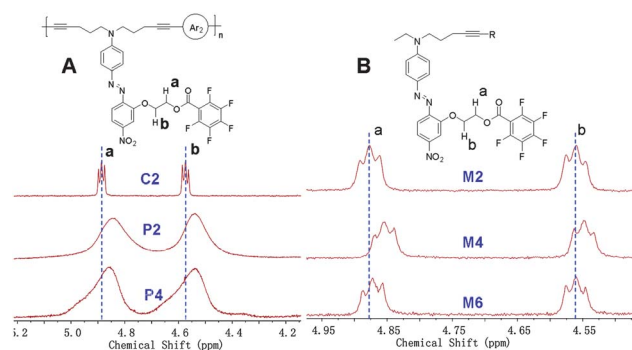


Fig. 2 ^1H NMR spectra of compounds containing pentafluorophenyl groups. A: polymers and monomers; B: model molecules.

the ^1H NMR spectrum (Fig. 2B) of M4 or M6, respectively. Thus, from their ^1H NMR spectra, a preliminary conclusion could be obtained: in this case, the self-assembly was present between the isolation groups and polymer main chain; the self-assembly effect between pentafluorophenyl and TPA was stronger than that between pentafluorophenyl and phenyl moieties; the self-assembly effects in the polymers were stronger than those in small molecules.

In their ^{13}C NMR spectra a similar phenomenon was observed. The $\text{C}=\text{O}$ groups should show a characteristic peak at about 160 ppm. In the ^{13}C NMR spectra of C1, P1, P3, and even the model molecules M1, M3 and M5, the chemical shifts of that peak were all at about 166 ppm. In the ^{13}C NMR spectrum of C2 was at 158.9 ppm, while after polymerization, it was at 154.7 ppm in P2, while still about 159 ppm in P4. As we know, it is much more difficult to measure the ^{13}C NMR spectra of polymers than small molecules, due to their special structure and relative poor solubility. Thus, this changes should be more obvious in the ^{13}C NMR spectra of model molecules. In the ^{13}C NMR spectrum of M2, the chemical shift was nearly the same as in C2, at 158.6 ppm. After the Sonogashira reaction, it was at 154.2 or 154.3 ppm in the ^{13}C NMR spectrum (Fig. S24 and S28) of M4 or M6, respectively. This could further confirm our speculations.

On the other hand, it was known in theory that pentafluorophenyl groups only have three types of F atom, and there should only be three peaks observed in the corresponding ^{19}F NMR spectra. However, the Ar–Ar^F self-assembly effect might change the environment of some F atoms. Therefore, if the Ar–Ar^F self-assembly effect was strong enough, additional peaks should also be observed in their ^{19}F NMR spectra. As shown in Fig. 3, along with the three original peaks, there were still some more peaks appearing in the ^{19}F NMR spectra of P2 and P4, and the intensity in P2 was stronger than that in P4. In the ^{19}F NMR spectra of the model molecules (Fig. 3), there were only three peaks in that of M2, while two more very weak peaks were observed in that of M4 and M6 after the Sonogashira coupling reaction, indicating that the self-assembly was between the isolation groups and polymer main chain, which is consistent with the results of the ^1H NMR.

The molecular weights of polymers were determined by gel permeation chromatography (GPC) with THF as an eluent and polystyrene standards as calibration standards. As shown in Table 1 and the experimental section, P1 and P2 showed slightly lower molecular weights than P3 and P4, possibly caused by the

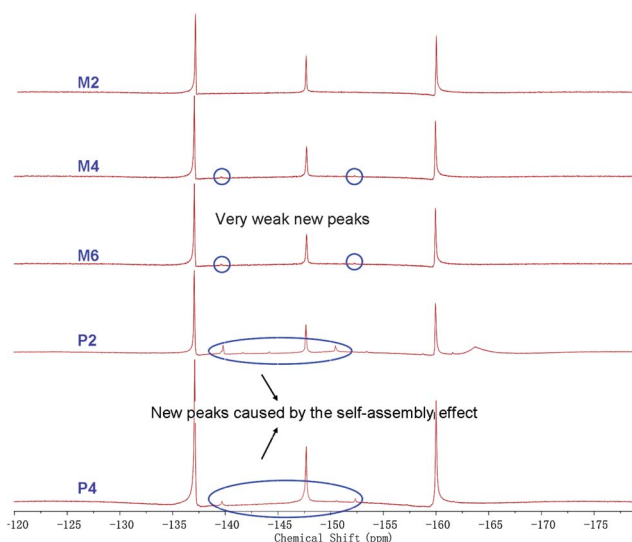


Fig. 3 ^{19}F NMR spectra of **P2**, **P4** and their model molecules.

lower reaction activity of aryl bromide. This lower reactive activity also made the yields of **P1** and **P2** much lower than those of **P3** and **P4**. Interestingly, **P2** and **P4** also exhibited slightly lower molecular weights than their corresponding polymers **P1** and **P3**, indicating that the introduction of perfluoroaromatic rings would make the activity of the Sonogashira reaction a little lower. However, the molecular weights of these four polymers were on the same level, around $10\,000\text{ g mol}^{-1}$, which would facilitate the comparison of their properties on the same level.

The TGA thermograms are shown in Fig. S29 (ESI †), and the 5% weight loss temperature (T_d) of the polymers is listed in Table 1. All the polymers were thermally stable with T_d values higher than $200\text{ }^{\circ}\text{C}$. **P2** and **P4** exhibited a little worse thermal stability than **P1** and **P3**, indicating that the pentafluorophenyl group was not as stable. But this was still good enough for NLO materials, because the temperatures for their real application are generally lower than $200\text{ }^{\circ}\text{C}$. The glass transition temperatures (T_g) of the polymers were also investigated using a differential scanning calorimeter (DSC), with the results summarized in Table 1. **P1** exhibited a T_g value of $73\text{ }^{\circ}\text{C}$, while the T_g value of **P2** increased to a large degree (up to $139\text{ }^{\circ}\text{C}$), indicating that the self-assembly effect existed in **P2**, as is consistent with other phenomena.

The UV-vis absorption spectra of the chromophores and polymers in different solvents are displayed in Fig. S30–S35 (ESI †),

Table 1 Characterization data of polymers

No.	Yield (%)	M_w^a	M_w/M_n^a	T_g^b ($^{\circ}\text{C}$)	T_d^c ($^{\circ}\text{C}$)
P1	51.3	9600	1.50	73	248
P2	30.7	8900	1.56	139	215
P3	68.6	11 400	1.97	(—) ^d	252
P4	68.0	9900	1.76	77	222

^a Determined by GPC in THF on the basis of a polystyrene calibration.

^b Glass transition temperature (T_g) of polymers detected by the DSC analyses under argon at a heating rate of $10\text{ }^{\circ}\text{C min}^{-1}$. ^c The 5% weight loss temperature of polymers detected by the TGA analyses under nitrogen at a heating rate of $10\text{ }^{\circ}\text{C min}^{-1}$. ^d Not obtained.

and the maximum absorption wavelengths (λ_{max}) for the π – π^* transition of the azo moieties in them are listed in Table 2. All the polymers exhibited similar λ_{max} values, nearly identical to their corresponding chromophores. This phenomenon indicated that the self-assembly effect did not occur between perfluoroaromatic rings and chromophore moieties, else the λ_{max} for **P2** and **P4** should be different from those of **P1** and **P3**. Thus, the self-assembly effect should only be present between isolation groups and polymer main chains as the ^1H NMR spectra disclosed.

NLO properties

In the excellent work of Jen and co-workers, the complementary Ar–Ar^F interactions could improve the poling efficiency of the dendron-substituted NLO chromophores, leading to the enhanced NLO activities.⁶ As mentioned above, it was confirmed that the Ar–Ar^F self-assembly effect could exist between the isolation groups and polymer main chains. Thus, how about this Ar–Ar^F self-assembly effect? To answer this question, the NLO activity of them should be measured. To evaluate the NLO activity of the polymers, their poled thin films were prepared. Due to its bad processability, **P1** could not form high-quality thin films through spin-coating. Therefore, its NLO coefficient was also tested in the doped PMMA film with the concentration of 50% (w/w). The most convenient technique to study the second-order NLO activity was to investigate the second harmonic generation (SHG) processes characterized by d_{33} , an SHG coefficient. To check the reproducibility, we repeated the measurements at least three times for each sample. Calculation of the SHG coefficients (d_{33}) for the poled films is based on the following equation:¹⁰

$$\frac{d_{33,s}}{d_{11,q}} = \frac{\chi_s^{(2)}}{\chi_q^{(2)}} = \sqrt{\frac{I_s}{I_q} \frac{l_{c,q}}{l_s}} F$$

where $d_{11,q}$ is the d_{11} of the quartz crystals, which is equal to 0.45 pm V^{-1} . I_s and I_q are the SHG intensities of the sample and the quartz, respectively, $l_{c,q}$ is the coherent length of the quartz, l_s is the thickness of the polymer film, and F is the correction factor of the apparatus and is equal to 1.2 when l_c is much greater than l_s . From the experimental data, the d_{33} values of **P1**–**P4** were calculated at a fundamental wavelength of 1064 nm (Table 3). Generally, the d_{33} value of the same NLO polymer could be different when measured by different methods or different testing systems at different times. To avoid the above-mentioned

Table 2 The maximum absorption of polymers and their corresponding chromophores (λ_{max} , nm)^a

	THF	1,4-Dioxane	CHCl_3	CHCl_2	DMF	DMSO	Film
P1	497	477	488	490	497	504	508
P2	491	476	488	488	496	499	500
P3	496	479	491	493	503	507	503
P4	494	482	496	496	501	508	504
C1	489	478	493	494	500	507	
C2	489	479	493	495	500	507	

^a The maximum absorption wavelength of the polymer (chromophore molecule) solutions with the concentrations fixed at 0.02 mg mL^{-1} ($2.5 \times 10^{-5}\text{ mol mL}^{-1}$).

possible deviations, the NLO properties of all the polymers were tested at the same time.

It was well-known that in theory, under identical experimental conditions, the NLO activities were proportional to the density of the chromophore moieties.¹¹ In **P1**, the comonomer unit of TPA, which is much larger than the phenyl one in **P3**, resulted in a much lower loading density of the chromophore moieties than that in **P3** (0.383 vs. 0.487). Therefore, the d_{33} value of **P1** (21.4 pm V⁻¹) was lower than that of **P3** (50.4 pm V⁻¹), since their structures were similar. The d_{33} values of the polymers **P2** and **P4**, with the pentafluorophenyl groups as isolation groups, were much higher than the corresponding polymers with phenyl as the isolation moieties, although they possessed a relatively lower loading density of the azo chromophore moieties than those in **P1** and **P3**, respectively. This should be ascribed to the presence of the self-assembly effect. As mentioned above, it was confirmed that the Ar–Ar^F self-assembly effect in **P2** using TPA as comonomer was stronger than that in **P4**, thus, from **P1** to **P2**, the d_{33} value increased more than 6 times, while the d_{33} value of **P4** was only 3.3 times of **P3**. Excitingly, the d_{33} value of **P4** reached up to 166.7 pm V⁻¹, which is, to the best of our knowledge, the highest value so far for linear polymers using simple azobenzenes as chromophore moieties.

As there might be some resonant enhancement¹² due to the absorption of the chromophore moieties at 532 nm, the NLO properties of **P1–P4** should be much smaller as shown in Table 3 ($d_{33}(\infty)$), which were calculated by using the approximate two-level model. Since all the polymers exhibited nearly the same UV-vis absorption behavior, their $d_{33}(\infty)$ values demonstrated the same phenomena as their d_{33} values.

To further study the alignment behavior of the chromophore moieties in the polymers, the order parameter (Φ) of the polymers (Table 3) was measured and calculated from the change of the UV-vis spectra of their films before and after poling under an electric field (Fig. 4 and S36[†]), according to the equation described in Table 3 (footnote e). The tested Φ values of **P2** (0.15) and **P4** (0.24) were still higher than those of **P1** (0.08) and **P3** (0.11), indicating the better alignment of the chromophore moieties in the poled film of **P2** and **P4**, further confirming the advantages of the self-assembly effect in NLO polymers.

The dynamic thermal stabilities of the NLO activities of the polymers were investigated by depoling experiments, in which the real-time decays of their SHG signals were monitored as the poled films were heated from 40 to 130 °C in air at a rate of 4 °C

Table 3 NLO activities of hyperbranched polymers

No.	T_e^a (°C)	l_s^b (μm)	d_{33}^c (pm V ⁻¹)	$d_{33(\infty)}^d$ (pm V ⁻¹)	Φ^e	N^f
P1	85	0.32	12.3	0.8	(—)	0.383
P1^g	105	0.36	21.4	1.5	0.08	
P2	130	0.27	128.5	11.7	0.15	0.342
P3	90	0.25	50.4	4.2	0.11	0.487
P4	95	0.28	166.7	13.7	0.24	0.425

^a The best poling temperature. ^b Film thickness. ^c Second harmonic generation (SHG) coefficient. ^d The nonresonant d_{33} values calculated by using the approximate two-level model. ^e Order parameter $\Phi = 1 - A_1/A_0$, A_1 and A_0 are the absorbance of the polymer film after and before corona poling, respectively. ^f The loading density of the effective chromophore moieties. ^g Tested in the doped PMMA film with the concentration of 50% (w/w).

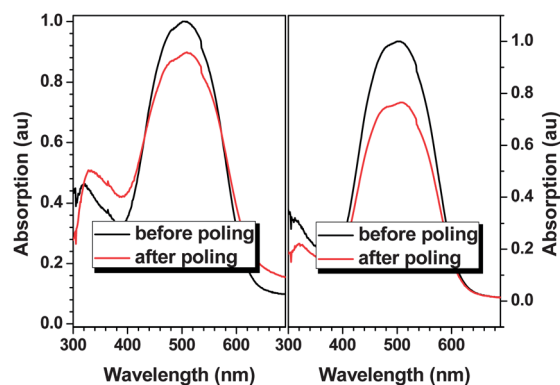


Fig. 4 Absorption spectra of the film of **P3** (left) and **P4** (right) before and after poling.

min⁻¹. Fig. 5 shows the decay of the SHG coefficient of **P1–P4** as a function of temperature. It is very easy to see that the onset temperatures for the decay of **P2** and **P4** with the pentafluorophenyl groups as the isolated groups, were much higher than their corresponding polymers with phenyl as the isolation moieties, especially **P2**, its onset temperatures for the decays reached up to 104 °C. That is to say, to destroy the alignment of the chromophore moieties in **P2** and **P4**, much more energy should be needed, indicating that the Ar–Ar^F self-assembly effect was still present after poling, and these interactions could increase the stability of NLO polymers, which could contribute to their practical application in the photonics field.

Thus, all the NLO behavior (including the poling and depoling experiments) of **P2** and **P4** confirmed the poling procedure of NLO materials with the self-assembly effect derived from Ar–Ar^F interactions, is a little different to the normal poling procedure (Fig. 6). Before poling, the chromophores were randomly arranged; when the temperature increased, the self-assembly effect from the Ar–Ar^F interactions was broken, if the electric field was applied at that time, the chromophore could be induced to a noncentrosymmetric alignment; after cooling, the self-assembly effect could be resumed, which could improve the stability of the NLO effect. It should be noted that the self-assembly effect was always present both before and after poling. Without poling, the self-assembly effect was present, but had nothing to do with the orderly alignment of the chromophore

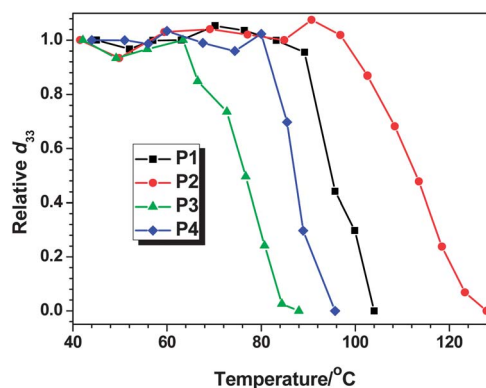


Fig. 5 Decay curves of the SHG coefficients of **P1–P4** as a function of the temperature.

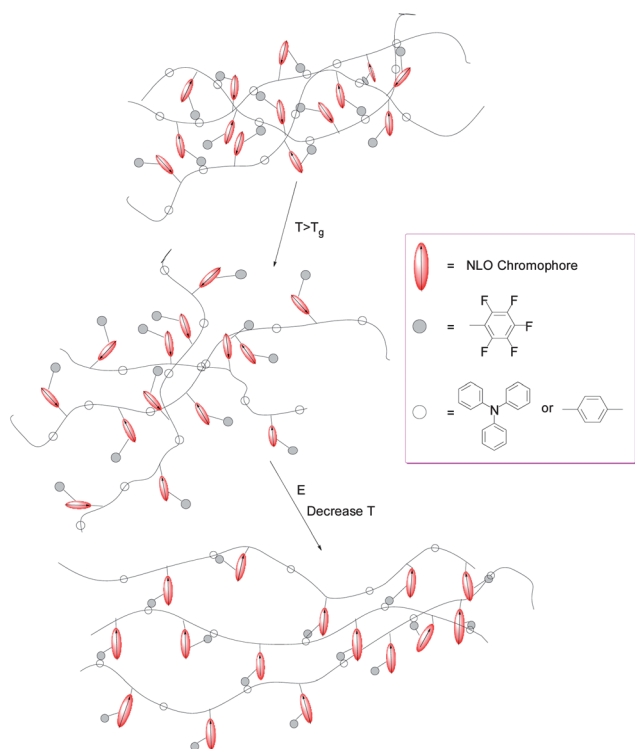


Fig. 6 Graphical illustration of the alignment formation of self-assembled polymer **P2** and **P4** by Ar–Ar^F interactions.

moieties. However, during the poling process, the self-assembly effect could benefit the noncentrosymmetric alignment of the chromophore moieties, thus, leading to the enhanced macroscopic NLO effect and the improved stability of the NLO effect.

Conclusions

In this paper, a facile route was designed to prepare four new NLO polyaryleneethynylenes **P1–P4** containing normal aromatic rings or perfluoroaromatic rings as isolation groups *via* a simple Sonogashira coupling reaction. Thanks to the Ar–Ar^F self-assembly effect, the d_{33} values and NLO stabilities of **P2** and **P4** with the pentafluorophenyl groups as isolated groups were much higher those of **P1** and **P3**. The d_{33} value of **P4** reached up to 166.7 pm V⁻¹, which is, to the best of our knowledge, the highest value so far for linear polymers using simple azobenzene as chromophore moieties. Thus, our successful example might stimulate the utilization of the Ar–Ar^F self-assembly effect, to construct new functional materials with good performance.

Experimental

Materials

Tetrahydrofuran (THF) was dried over and distilled from K–Na alloy under an atmosphere of dry nitrogen. Triethylamine (Et₃N) was distilled under normal pressure and kept over potassium hydroxide. Dichloromethane (CH₂Cl₂, DCM) was dried over CaH₂ and distilled under normal pressure before use. *N,N*-Di-(4-pentynyl)benzenamine (**S1**), diazonium fluoroborate **S2** and *N*-ethyl-*N*-(4-pentynyl)benzenamine (**S4**) were prepared in our

previous work.^{7,8a} 1,4-Diiodobenzene was purchased from Alfa Aesar. All other reagents were used as received.

Instrumentation

¹H NMR spectra were measured on a Varian Mercury300 or Bruker ARX 400 spectrometer using tetramethylsilane (TMS; $\delta = 0$ ppm) as an internal standard. The Fourier transform infrared (FTIR) spectra were recorded on a PerkinElmer-2 spectrometer in the region of 3000–400 cm⁻¹. UV-vis spectra were obtained using a Shimadzu UV-2550 spectrometer. Elemental analyses (EA) were performed by a CARLOERBA-1106 microelemental analyzer. Gel permeation chromatography (GPC) was used to determine the molecular weights of polymers. GPC analysis was performed on a Waters HPLC system equipped with a 2690D separation module and a 2410 refractive index detector. Polystyrene standards were used as calibration standards for GPC. THF was used as an eluent, and the flow rate was 1.0 mL min⁻¹. Thermal analysis was performed on NETZSCH STA449C thermal analyzer at a heating rate of 10 °C min⁻¹ in nitrogen at a flow rate of 50 cm³ min⁻¹ for thermogravimetric analysis (TGA) and the thermal transitions of the polymers. The thickness of the films was measured with an Ambios Technology XP-2 profilometer.

Synthesis of chromophore S3

N,N-Di(4-pentynyl)benzenamine (**S1**) (901.3 mg, 4.0 mmol) and diazonium salt **S2** (1.19 g, 4.0 mmol) were dissolved in 8 mL DMF/THF (1/1, v/v) at 0 °C. The reaction mixture was stirred for 12 h at 0 °C, and then treated with H₂O, extracted with CH₂Cl₂, and washed with brine. The organic layer was dried over anhydrous sodium sulfate. After removal of the organic solvent, the crude product was purified by column chromatography on silica gel using ethyl acetate/petroleum ether (b.p. 60–90 °C)(2/1, v/v) as the eluent to afford a deep red solid (1.1 g, 63.3%). ¹H NMR (400 MHz, CDCl₃, 298 K), δ (TMS, ppm): 1.88 (m, 4H, –CH₂–), 2.05 (s, 2H, –C≡C–H), 2.30 (m, 4H, –CH₂–), 3.59 (t, $J = 6.0$ Hz, 4H, –NCH₂–), 4.00 (t, $J = 4.0$ Hz, 2H, –OCH₂–), 4.37 (t, $J = 4.0$ Hz, 2H, –OCH₂–), 6.80 (d, $J = 8.0$ Hz, 2H, ArH), 7.72 (d, $J = 8.0$ Hz, 1H, ArH), 7.86 (d, $J = 8.0$ Hz, 2H, ArH) 7.95 (m, 2H, ArH).

General procedure for the synthesis of chromophore C1 and C2

Chromophore **S3** (1.00 equiv.), carboxyl-containing compound (1.50 equiv.), 1-(3-dimethylaminopropyl)-3-ethylcarbodiimide hydrochloride (EDC) (2.00 equiv.), and 4-(*N,N*-dimethyl)aminopyridine (DMAP) (0.20 equiv.) were dissolved in dry CH₂Cl₂ (0.1 mmol mL⁻¹ of chromophore **S3**) and stirred at room temperature for 3 h, and then treated with a saturated solution of citric acid and extracted with CH₂Cl₂, and washed with a saturated solution of citric acid and brine. After removing all the solvent and the crude product was purified by column chromatography on silica gel.

Chromophore C1. Chromophore **S3** (499.7 mg, 1.15 mmol), benzoic acid (211.3 mg, 1.73 mmol). The crude product was purified by column chromatography on silica gel using ethyl acetate/chloroform (1/20, v/v) as eluent to afford deep red solid (614.3 mg, 99.2%). IR (KBr), ν (cm⁻¹): 3267 (C≡C–H), 1711

(C=O), 1519, 1335 (–NO₂). ¹H NMR (400 MHz, CDCl₃, 298 K), δ (TMS, ppm): 1.87 (m, 4H, –CH₂–), 2.06 (s, 2H, –C≡C–H), 2.30 (m, 4H, –CH₂–), 3.58 (t, *J* = 8.0 Hz, 4H, –NCH₂–), 4.62 (t, *J* = 4.0 Hz, 2H, –OCH₂–), 4.80 (t, *J* = 4.0 Hz, 2H, –COOCH₂–), 6.74 (d, *J* = 8.0 Hz, 2H, ArH), 7.40 (t, *J* = 8.0 Hz, 2H, ArH), 7.55 (t, *J* = 8.0 Hz, 1H, ArH), 7.69 (d, *J* = 8.0 Hz, 1H, ArH), 7.86 (d, *J* = 8.0 Hz, 1H, ArH), 7.92 (m, 1H, ArH), 8.05 (m, 3H, ArH), 8.17 (d, *J* = 8.0 Hz, 1H, ArH). ¹³C NMR (75 MHz, CDCl₃, 298 K), δ (TMS, ppm): 49.5, 61.7, 64.1, 67.9, 101.0, 110.2, 111.6, 117.3, 126.0, 128.7, 130.7, 137.6, 144.8, 147.0, 148.0, 150.7, 154.5, 165.7. C₃₁H₃₀N₄O₅ (EA) (found/calcd): C, 68.77/69.13; H, 6.06/5.61; N, 10.06/10.40%.

Chromophore C2. Chromophore S3 (499.7 mg, 1.15 mmol), pentafluorobenzoic acid (365.8 mg, 1.73 mmol). The crude product was purified by column chromatography on silica gel using ethyl acetate/chloroform (1/20, v/v) as the eluent to afford a deep red solid (686.2 mg, 94.9%). IR (KBr), *v* (cm^{–1}): 3299 (C≡C–H), 1743 (C=O), 1516, 1336 (–NO₂). ¹H NMR (400 MHz, CDCl₃, 298 K), δ (TMS, ppm): 1.87 (m, 4H, –CH₂–), 2.05 (s, 2H, –C≡C–H), 2.30 (m, 4H, –CH₂–), 3.58 (t, *J* = 8.0 Hz, 4H, –NCH₂–), 4.56 (t, *J* = 4.0 Hz, 2H, –OCH₂–), 4.88 (t, *J* = 4.0 Hz, 2H, –COOCH₂–), 6.76 (d, *J* = 8.0 Hz, 2H, ArH), 7.69 (d, *J* = 8.0 Hz, 1H, ArH), 7.83 (d, *J* = 8.0 Hz, 2H, ArH), 7.94 (m, 2H, ArH). ¹³C NMR (75 MHz, CDCl₃, 298 K), δ (TMS, ppm): 15.9, 25.7, 49.9, 64.2, 67.9, 69.4, 83.0, 110.2, 111.2, 117.5, 126.3, 144.1, 147.5, 147.8, 151.1, 154.4, 158.9. C₃₁H₂₅N₄O₅F₅ (EA) (found/calcd): C, 59.24/59.66; H, 3.95/4.01; N, 8.91/8.91%.

General procedure for the synthesis of P1–P4

A mixture of chromophore C1 or C2 (1.00 equiv.), aryl halide (1.00 equiv.), copper iodide (CuI) (5 mol%), triphenylphosphine (PPh₃) (5 mol%), tetrakis(triphenylphosphine)palladium (Pd(PPh₃)₄) (3 mol%), was carefully degassed and charged with argon. THF (monomer C1 or C2 concentration was about 0.025 mmol mL^{–1})/Et₃N (3/1 by volume) was then added. The reaction was stirred for 4 days at an appropriate temperature. The mixture was passed through a cotton filter and dropped into a large volume of methanol. The precipitate was collected, further purified by several precipitations of its THF solution into acetone, and dried in a vacuum at 40 °C to a constant weight.

P1. Chromophore C1 (80.8 mg, 0.15 mmol), *N,N*-bis(4-bromophenyl)benzenamine (60.5 mg, 0.15 mmol), reaction temperature: 60 °C. P1 was obtained as a deep red powder (60.0 mg, 51.3%). *M_w* = 9600, *M_w*/*M_n* = 1.50 (GPC, polystyrene calibration). IR (KBr), *v* (cm^{–1}): 1718 (C=O), 1515, 1337 (–NO₂). ¹H NMR (300 MHz, CDCl₃, 298 K), δ (TMS, ppm): 1.6–2.1 (–CH₂–), 2.1–2.6 (–CH₂–), 3.1–3.8 (–NCH₂–), 4.3–4.8 (–OCH₂– and –COOCH₂–), 6.4–6.8 (ArH), 7.0–8.1 (ArH). ¹³C NMR (75 MHz, CDCl₃, 298 K), δ (TMS, ppm): 17.10, 26.10, 50.35, 63.36, 66.48, 68.94, 111.06, 111.78, 117.79, 126.60, 128.61, 129.98, 132.76, 133.34, 144.67, 147.75, 148.25, 151.20, 155.09, 166.60.

P2. Chromophore C2 (94.3 mg, 0.15 mmol), *N,N*-bis(4-bromophenyl)benzenamine (60.5 mg, 0.15 mmol), reaction temperature: 60 °C. P2 was obtained as a deep red powder (40.2 mg, 30.7%). *M_w* = 8900, *M_w*/*M_n* = 1.56 (GPC, polystyrene

calibration). IR (KBr), *v* (cm^{–1}): 1739 (C=O), 1515, 1336 (–NO₂). ¹H NMR (300 MHz, CDCl₃, 298 K), δ (TMS, ppm): 1.7–2.2 (–CH₂–), 2.3–2.6 (–CH₂–), 3.1–3.8 (–NCH₂–), 4.4–4.6 (–OCH₂–), 4.7–5.0 (–COOCH₂–), 6.4–7.0 (ArH), 7.0–8.0 (ArH). ¹³C NMR (75 MHz, CDCl₃, 298 K), δ (TMS, ppm): 17.04, 26.05, 50.35, 64.45, 66.34, 68.24, 110.64, 111.61, 117.80, 126.53, 148.20, 154.72.

P3. Chromophore C1 (107.7 mg, 0.20 mmol), 1,4-diiodobenzene (66.0 mg, 0.20 mmol), reaction temperature: 30 °C. P3 was obtained as a deep red powder (83.9 mg, 68.6%). *M_w* = 11 400, *M_w*/*M_n* = 1.97 (GPC, polystyrene calibration). IR (KBr), *v* (cm^{–1}): 1719 (C=O), 1516, 1336 (–NO₂). ¹H NMR (300 MHz, CDCl₃, 298 K), δ (TMS, ppm): 1.2–2.1 (–CH₂–), 2.2–2.6 (–CH₂–), 3.3–3.7 (–NCH₂–), 4.2–4.8 (–OCH₂– and –COOCH₂–), 6.5–6.8 (ArH), 7.0–7.2 (ArH), 7.2–8.2 (ArH). ¹³C NMR (75 MHz, CDCl₃, 298 K), δ (TMS, ppm): 17.30, 26.33, 29.94, 32.45, 50.53, 63.38, 68.89, 81.64, 90.45, 110.94, 111.73, 117.80, 123.22, 126.63, 128.60, 129.98, 131.69, 132.24, 133.34, 137.69, 144.57, 148.15, 151.35, 155.06, 160.75, 166.63.

P4. Chromophore C2 (113.1 mg, 0.18 mmol), 1,4-diiodobenzene (59.4 mg, 0.18 mmol). P4 was obtained as a deep red powder (86.1 mg, 68.0%). *M_w* = 9900, *M_w*/*M_n* = 1.76 (GPC, polystyrene calibration). IR (KBr), *v* (cm^{–1}): 1740 (C=O), 1517, 1335 (–NO₂). ¹H NMR (300 MHz, CDCl₃, 298 K), δ (TMS, ppm): 1.8–2.2 (–CH₂–), 2.3–2.7 (–CH₂–), 3.4–3.8 (–NCH₂–), 4.4–4.7 (–OCH₂–), 4.7–5.0 (–COOCH₂–), 6.7–7.0 (ArH), 7.1–8.0 (ArH). ¹³C NMR (75 MHz, CDCl₃, 298 K), δ (TMS, ppm): 17.28, 26.34, 50.49, 64.47, 68.39, 81.59, 90.65, 107.91, 110.81, 111.62, 117.82, 123.24, 126.55, 128.75, 131.64, 132.32, 133.27, 136.95, 137.68, 138.62, 144.53, 144.93, 146.63, 147.84, 148.17, 151.50, 154.72, 159.10.

Synthesis of chromophore S5

N-Ethyl-*N*-(4-pentynyl)benzenamine (S4) (1.34 g, 4.5 mmol) and diazonium salt S2 (1.34 g, 4.5 mmol) were dissolved in 8 mL DMF/THF (1/1, v/v) at 0 °C. The reaction mixture was stirred for 12 h at 0 °C, and then treated with H₂O and extracted with CH₂Cl₂, washed with brine. The organic layer was dried over anhydrous sodium sulfate. After removal of the organic solvent, the crude product was purified by column chromatography on silica gel using ethyl acetate/petroleum ether (2/1, v/v) as the eluent to afford a deep red solid (1.62 g, 81.8%). IR (KBr), *v* (cm^{–1}): 3534 (–OH), 3218 (C≡C–H), 1519, 1335 (–NO₂). ¹H NMR (300 MHz, CDCl₃, 298 K), δ (TMS, ppm): 1.25 (t, *J* = 6.6 Hz, 3H, –CH₃), 1.89 (m, 2H, –CH₂–), 2.08 (s, 1H, C≡CH), 2.31 (m, 2H, –CH₂–), 3.46–3.57 (m, 5H, –NCH₂– and –OH), 3.99 (s, br, 2H, –OCH₂–), 4.37 (t, *J* = 4.2 Hz, 2H, –OCH₂–), 6.77 (d, *J* = 9.0 Hz, 2H, ArH), 7.72 (d, *J* = 9.6 Hz, H, ArH), 7.86 (d, *J* = 9.6 Hz, 2H, ArH), 7.95 (m, 2H, ArH). ¹³C NMR (75 MHz, CDCl₃, 298 K), δ (ppm): 12.27, 15.84, 25.89, 45.43, 49.14, 60.72, 69.43, 72.32, 83.03, 110.64, 111.07, 117.17, 117.69, 126.46, 143.59, 147.35, 147.61, 151.23, 154.38.

General procedure for the synthesis of model molecules M1 and M2

Chromophore S5 (1.00 equiv.), carboxyl-containing compound (1.50 equiv.), 1-(3-dimethylaminopropyl)-3-ethylcarbodiimide

hydrochloride (EDC) (2.00 equiv.), and 4-(*N,N*-dimethyl)aminopyridine (DMAP) (0.20 equiv.) were dissolved in dry CH₂Cl₂ (0.1 mmol mL⁻¹ of chromophore **S5**) and stirred at room temperature for 3 h, and then treated with saturated solution of citric acid and extracted with CH₂Cl₂, and washed with a saturated solution of citric acid and brine. After removal of all the solvent, the crude product was purified by column chromatography on silica gel.

Chromophore M1. Chromophore **S5** (396 mg, 1.0 mmol), benzoic acid (183 mg, 1.5 mmol). The crude product was purified by column chromatography on silica gel using ethyl acetate/chloroform (1/20, v/v) as the eluent to afford a deep red solid (472 mg, 94.4%). IR (KBr), ν (cm⁻¹): 3270 (C≡C-H), 1713 (C=O), 1519, 1335 (-NO₂). ¹H NMR (300 MHz, CDCl₃, 298 K), δ (TMS, ppm): 1.24 (t, *J* = 6.9 Hz, 3H, -CH₃), 1.88 (m, 2H, -CH₂-), 2.06 (s, 1H, -C≡CH), 2.30 (m, 2H, -CH₂-), 3.50 (m, 4H, -NCH₂-), 4.62 (t, *J* = 5.7 Hz, 2H, -O-CH₂-), 4.79 (t, *J* = 5.7 Hz, 2H, -COOCH₂-), 6.70 (d, *J* = 8.4 Hz, 2H, ArH), 7.40 (m, 2H, ArH), 7.57 (m, 1H, ArH), 7.71 (d, *J* = 8.7 Hz, 1H, ArH), 7.86 (d, *J* = 9.0 Hz, ArH), 7.92 (d, 1H, ArH), 7.99–8.07 (m, 3H, ArH). ¹³C NMR (75 MHz, CDCl₃, 298 K), δ (TMS, ppm): 12.33, 15.90, 25.96, 45.48, 49.20, 63.10, 68.60, 69.42, 83.085, 110.67, 111.13, 117.42, 126.41, 128.30, 129.70, 133.04, 144.06, 147.58, 147.74, 151.07, 154.71, 166.37.

Chromophore M2. Chromophore **S5** (515 mg, 1.3 mmol), pentafluorobenzoic acid (413 mg, 1.95 mmol). The crude product was purified by column chromatography on silica gel using ethyl acetate/chloroform (1/20, v/v) as the eluent to afford a deep red solid (632 mg, 82.4%). IR (KBr), ν (cm⁻¹): 3313 (C≡C-H), 1744 (C=O), 1518, 1334 (-NO₂). ¹H NMR (300 MHz, CDCl₃, 298 K), δ (TMS, ppm): 1.26 (t, *J* = 6.9 Hz, 3H, -CH₃), 1.89 (m, 2H, -CH₂-), 2.07 (s, 1H, -C≡CH), 2.30 (m, 2H, -CH₂-), 3.53 (m, 4H, -NCH₂-), 4.56 (t, *J* = 4.5 Hz, 2H, -OCH₂-), 4.88 (t, *J* = 4.5 Hz, 2H, -COOCH₂-), 6.73 (d, *J* = 9.0 Hz, 2H, ArH), 7.69 (d, *J* = 9.0 Hz, 1H, ArH), 7.83 (d, *J* = 9.0 Hz, 2H, ArH), 7.94 (m, 2H, ArH). ¹³C NMR (75 MHz, CDCl₃, 298 K), δ (TMS, ppm): 12.03, 15.68, 25.76, 45.29, 49.01, 64.04, 67.79, 69.21, 82.96, 110.11, 110.79, 117.16, 117.26, 126.12, 143.73, 147.30, 147.48, 150.97, 154.21, 158.65.

General procedure for the synthesis of M3–M6

A mixture of chromophore **M1** or **M2** (1.10 equiv.), aryl halides (1.00 equiv.), copper iodide (CuI) (5 mol%), triphenylphosphine (PPh₃) (5 mol%), tetrakis(triphenylphosphine)palladium (Pd(PPh₃)₄) (3 mol%), was carefully degassed and charged with argon. THF (the concentration **M1** or **M2** was about 0.025 mmol mL⁻¹)/Et₃N (3/1 by volume) was then added. The reaction was stirred for 2 days at room temperature, and then treated with a saturated solution of citric acid and extracted with CH₂Cl₂, and washed with a saturated solution of citric acid and brine. After removal of all the solvent, the crude product was purified by column chromatography on silica gel.

M3. Chromophore **M1** (106 mg, 0.21 mmol), 4-iodo-*N,N*-diphenylaniline (61 mg, 0.165 mmol). The crude product was purified by column chromatography on silica gel using ethyl

acetate/chloroform (1/35, v/v) as the eluent to afford a deep red solid (45 mg, 36.9%). IR (KBr), ν (cm⁻¹): 1721 (C=O), 1515, 1336 (-NO₂). ¹H NMR (300 MHz, CDCl₃, 298 K), δ (TMS, ppm): 1.25 (t, *J* = 6.9 Hz, 3H, -CH₃), 1.95 (m, 2H, -CH₂-), 2.51 (t, *J* = 6.3 Hz, 2H, -CH₂-), 3.52–3.58 (m, 4H, -NCH₂-), 4.61 (t, *J* = 4.5 Hz, 2H, -OCH₂-), 4.78 (t, *J* = 4.8 Hz, 2H, -COOCH₂-), 6.73 (d, *J* = 9.6 Hz, 2H, ArH), 6.97–7.09 (m, 7H, ArH), 7.26 (m, 7H, ArH), 7.39 (m, 2H, ArH), 7.54 (m, H, ArH), 7.70 (d, *J* = 8.7 Hz, 1H, ArH), 7.84–8.05 (m, 6H, ArH). ¹³C NMR (75 MHz, CDCl₃, 298 K), δ (TMS, ppm): 12.42, 17.01, 26.46, 29.66, 45.56, 49.47, 63.11, 68.67, 81.68, 87.61, 110.77, 111.20, 116.50, 117.45, 122.54, 122.34, 124.75, 126.45, 128.31, 129.31, 129.73, 132.35, 133.04, 144.09, 147.20, 147.75, 151.18, 154.73, 166.37.

M4. Chromophore **M2** (128 mg, 0.20 mmol), 4-iodo-*N,N*-diphenylaniline (61 mg, 0.165 mmol). The crude product was purified by column chromatography on silica gel using ethyl acetate/chloroform (1/50, v/v) as the eluent to afford a deep red solid (83 mg, 50.0%). IR (KBr), ν (cm⁻¹): 1741 (C=O), 1515, 1335 (NO₂). ¹H NMR (300 MHz, CDCl₃, 298 K), δ (TMS, ppm): 1.26 (t, *J* = 6.9 Hz, 3H, -CH₃), 1.96 (m, 2H, -CH₂-), 2.52 (t, *J* = 6.3 Hz, 2H, -CH₂-), 3.53–3.62 (m, 4H, -NCH₂-), 4.55 (t, *J* = 4.2 Hz, 2H, -OCH₂-), 4.86 (t, *J* = 4.2 Hz, 2H, -COOCH₂-), 6.76 (d, *J* = 9.0 Hz, 2H, ArH), 7.00–7.11 (m, 7H, ArH), 7.26 (7H, ArH), 7.69 (d, *J* = 9.3 Hz, 1H, ArH), 7.83 (d, *J* = 8.7 Hz, 2H, ArH), 7.93 (m, 2H, ArH). ¹³C NMR (75 MHz, CDCl₃, 298 K), δ (TMS, ppm): 12.26, 16.90, 26.33, 45.48, 49.36, 64.09, 67.91, 81.58, 87.59, 110.23, 110.97, 116.44, 117.41, 117.51, 122.44, 123.25, 124.66, 126.32, 129.25, 132.27, 143.87, 147.12, 147.40, 147.60, 151.16, 154.27.

M5. Chromophore **M1** (106 mg, 0.21 mmol), iodobenzene (34 mg, 0.165 mmol). The crude product was purified by column chromatography on silica gel using ethyl acetate/chloroform (1/35, v/v) as the eluent to afford a deep red solid (38 mg, 40.0%). IR (KBr), ν (cm⁻¹): 1719 (C=O), 1517, 1335 (-NO₂). ¹H NMR (300 MHz, CDCl₃, 298 K), δ (TMS, ppm): 1.26 (t, *J* = 6.9 Hz, 3H, -CH₃), 1.96 (m, 2H, -CH₂-), 2.52 (t, *J* = 6.9 Hz, 2H, -CH₂-), 3.50–3.62 (m, 4H, -NCH₂-), 4.61 (t, *J* = 4.5 Hz, 2H, -OCH₂-), 4.79 (t, *J* = 4.5 Hz, 2H, -COOCH₂-), 6.74 (d, *J* = 9.6 Hz, 2H, ArH), 7.30 (m, 3H, ArH), 7.40 (m, 4H, ArH), 7.54 (m, H, ArH), 7.71 (d, *J* = 9.0 Hz, H, ArH), 7.91–8.06 (m, 4H, ArH). ¹³C NMR (75 MHz, CDCl₃, 298 K), δ (TMS, ppm): 12.38, 16.91, 26.33, 45.52, 49.40, 63.08, 68.63, 81.62, 88.63, 110.70, 111.16, 117.42, 123.43, 126.41, 127.81, 128.27, 129.67, 131.42, 133.01, 144.05, 147.58, 147.70, 151.12, 154.68, 166.32.

M6. Chromophore **M2** (118 mg, 0.20 mmol), iodobenzene (34 mg, 0.165 mmol). The crude product was purified by column chromatography on silica gel using ethyl acetate/chloroform (1/50, v/v) as the eluent to afford a deep red solid (69 mg, 51.2%). IR (KBr), ν (cm⁻¹): 1740 (C=O), 1520, 1335 (-NO₂). ¹H NMR (300 MHz, CDCl₃, 298 K), δ (TMS, ppm): 1.27 (t, *J* = 6.9 Hz, 3H, -CH₃), 1.96 (m, 2H, -CH₂-), 2.52 (t, *J* = 6.9 Hz, 2H, -CH₂-), 3.4–3.7 (m, 4H, -NCH₂-), 4.56 (t, *J* = 4.2 Hz, 2H, -OCH₂-), 4.87 (t, *J* = 4.2 Hz, 2H, -COOCH₂-), 6.77 (d, *J* = 9.3 Hz, 2H, ArH), 7.31 (m, 2H, ArH), 7.42 (m, 2H, ArH), 7.70 (d, *J* = 9.0 Hz, 2H, ArH), 7.84 (d, 2H, *J* = 9.0 Hz, ArH), 7.94 (m, 2H, ArH). ¹³C NMR (75 MHz, CDCl₃, 298 K), δ (TMS, ppm): 12.30, 16.90,

26.26, 45.52, 49.39, 64.18, 67.97, 81.61, 88.60, 110.34, 111.04, 117.60, 123.45, 126.37, 127.81, 128.26, 131.42, 143.95, 147.69, 151.22, 154.31.

Preparation of polymer thin films

The polymers (or P1 and PMMA mixture) were dissolved in THF (concentration ~3 wt%), and the solutions were filtered through syringe filters. Polymer films were spin coated onto indium-tin-oxide (ITO)-coated glass substrates, which were cleaned with DMF, acetone, distilled water, and THF sequentially in an ultrasonic bath before use. Residual solvent was removed by heating the films in a vacuum oven at 40 °C.

NLO measurements of the poled films

The measuring procedure was similar to those reported previously.^{13,14} The second-order optical nonlinearity of the polymers was determined by *in situ* second harmonic generation (SHG) experiment using a closed temperature-controlled oven with optical windows and three needle electrodes. The films were kept at 45° to the incident beam and poled inside the oven, and the SHG intensity was monitored simultaneously. Poling conditions were as follows: temperature, different for each polymer (Table 3); voltage, 7.8 kV at the needle point; gap distance, 0.8 cm. The SHG measurements were carried out with an Nd : YAG laser operating at a 10 Hz repetition rate and an 8 ns pulse width at 1064 nm. A Y-cut quartz crystal served as the reference.

Acknowledgements

We are grateful to the National Science Foundation of China (no. 21034006), and the Doctoral Fund of Ministry of Education of China (20090141110043) for financial support.

Notes and references

- (a) H. Zhang, F. Xin, Y. Li, A. Hao, W. An and T. Sun, *Prog. Chem.*, 2010, **22**, 2276; (b) K. Ariga and T. Kunitake, *Supramolecular Chemistry-fundamentals and Applications*, Springer-Verlag Berlin Heidelberg, 2006; (c) J. C. Sinclair, *Nat. Chem.*, 2012, **4**, 346; (d) S. I. Stupp, *Nano Lett.*, 2010, **10**, 4783; (e) J. D. Brodin, X. I. Ambroggio, C. Tang, K. N. Parent, T. S. Baker and F. A. Tezcan, *Nat. Chem.*, 2012, **4**, 375; (f) S. A. Woodson, *Acc. Chem. Res.*, 2011, **44**, 1312; (g) Y. Luo, W. Yu, F. Xu and L. Zhang, *J. Polym. Sci., Part A: Polym. Chem.*, 2012, **50**, 2052.
- (a) L. Zang, Y. Che and J. S. Moore, *Acc. Chem. Res.*, 2008, **41**, 1596; (b) B. K. An, J. Gierschner and S. Y. Park, *Acc. Chem. Res.*, 2012, **45**, 544; (c) S. H. Jang and A. K.-Y. Jen, *Chem.-Asian J.*, 2009, **4**, 20; (d) G. Salassa, M. J. J. Coenen, S. J. Wezengberg, B. L. M. Hendriksen, S. Speller, J. A. A. W. Elemans and A. W. Kleij, *J. Am. Chem. Soc.*, 2012, **134**, 7186; (e) J. H. Olivier, J. Barberá, E. Bahaidarah, A. Harriman and R. Ziessel, *J. Am. Chem. Soc.*, 2012, **134**, 6100.
- (a) C. R. Patrick and G. S. Prosser, *Nature*, 1960, **187**, 1021; (b) G. W. Coates, A. R. Dunn, L. M. Henling, D. A. Dougherty and R. H. Gubbs, *Angew. Chem., Int. Ed. Engl.*, 1997, **36**, 248.
- (a) D. M. Burland, R. D. Miller and C. A. Walsh, *Chem. Rev.*, 1994, **94**, 31; (b) Y. Bai, N. Song, J. P. Gao, X. Sun, X. Wang, G. Yu and Z. Y. Wang, *J. Am. Chem. Soc.*, 2005, **127**, 2060; (c) T. J. Marks and M. A. Ratner, *Angew. Chem., Int. Ed. Engl.*, 1995, **34**, 155; (d) D. Yu, A. Gharavi and L. P. Yu, *J. Am. Chem. Soc.*, 1995, **117**, 11680; (e) S. R. Marder, B. Kippelen, A. K. Y. Jen and N. Peyghambarian, *Nature*, 1997, **388**, 845; (f) M. Lee, H. E. Katz, C. Erben, D. M. Gill, P. Gopalan, J. D. Heber and D. J. McGee, *Science*, 2002, **298**, 1401; (g) Y. Shi, C. Zhang, H. Zhang, J. H. Bechtel, L. R. Dalton, B. H. Robinson, W. H. Steier and L. R. Dalton, *Science*, 2000, **288**, 119; (h) C. V. Mclaughlin, M. Hayden, B. Polishak, S. Huang, J. D. Luo, T.-D. Kim and A. K. Y. Jen, *Appl. Phys. Lett.*, 2008, **92**, 151107; (i) L. R. Dalton, P. A. Sullivan and D. H. Bale, *Chem. Rev.*, 2010, **110**, 25; (j) J. D. Luo, X. H. Zhou and A. K. Y. Jen, *J. Mater. Chem.*, 2009, **19**, 7410; (k) J. D. Luo, S. Huang, Z. W. Shi, B. M. Polishak, X. H. Zhou and A. K.-Y. Jen, *Chem. Mater.*, 2011, **23**, 544.
- (a) B. H. Robinson and L. R. Dalton, *J. Phys. Chem. A*, 2000, **104**, 4785; (b) B. H. Robinson, L. R. Dalton, H. W. Harper, A. Ren, F. Wang, C. Zhang, G. Todorova, M. Lee, R. Aniszfeld, S. Garner, A. Chen, W. H. Steier, S. Houbrecht, A. Persoons, I. Ledoux, J. Zyss and A. K.-Y. Jen, *Chem. Phys.*, 1999, **245**, 35.
- (a) T. D. Kim, J. Kang, J. Luo, S. Jang, J. Na, N. Tucker, J. B. Benedict, L. R. Dalton, T. Gray, R. M. Overney, D. H. Park, W. N. Herman and A. K.-Y. Jen, *J. Am. Chem. Soc.*, 2007, **129**, 488; (b) X. Zhou, J. Luo, S. Huang, T. Kim, Z. Shi, Y. Cheng, S. Jang, D. B. Knorr, R. M. Overney and A. K.-Y. Jen, *Adv. Mater.*, 2009, **21**, 1976.
- (a) Z. Li, Z. Li, C. Di, Z. Zhu, Q. Li, Q. Zeng, K. Zhang, Y. Liu, C. Ye and J. Qin, *Macromolecules*, 2006, **39**, 6951; (b) Q. Zeng, Z. Li, Z. Li, C. Ye, J. Qin and B. Z. Tang, *Macromolecules*, 2007, **40**, 5634; (c) Q. Li, Z. Li, F. Zeng, W. Gong, Z. Li, Z. Zhu, Q. Zeng, S. Yu, C. Ye and J. Qin, *J. Phys. Chem. B*, 2007, **111**, 508; (d) Z. Li, P. Li, S. Dong, Z. Zhu, Q. Li, Q. Zeng, Z. Li, C. Ye and J. Qin, *Polymer*, 2007, **48**, 3650; (e) Z. Li, S. Dong, G. Yu, Z. Li, Y. Liu, C. Ye and J. Qin, *Polymer*, 2007, **48**, 5520; (f) Z. Li, S. Dong, P. Li, Z. Li, C. Ye and J. Qin, *J. Polym. Sci., Part A: Polym. Chem.*, 2008, **46**, 2983; (g) Z. Li, G. Yu, W. Wu, Y. Liu, C. Ye, J. Qin and Z. Li, *Macromolecules*, 2009, **42**, 3864; (h) Z. Li, W. Wu, Q. Li, G. Yu, L. Xiao, Y. Liu, C. Ye, J. Qin and Z. Li, *Angew. Chem., Int. Ed.*, 2010, **49**, 2763; (i) W. Wu, L. Huang, C. Song, G. Yu, C. Ye, Y. Liu, J. Qin and Z. Li, *Chem. Sci.*, 2012, **3**, 1256; (j) Z. Li, Q. Li and J. Qin, *Polym. Chem.*, 2011, **2**, 2723.
- (a) Z. Li, A. Qin, J. W. Y. Lam, Y. Dong, C. Ye, I. Williams and B. Tang, *Macromolecules*, 2006, **39**, 1436; (b) Z. Zhu, Z. Li, Y. Tan, Z. Li, Q. Li, C. Ye and J. Qin, *Polymer*, 2006, **47**, 7881.
- (a) Z. Li, G. Yu, P. Hu, C. Ye, Y. Liu, J. Qin and Z. Li, *Macromolecules*, 2009, **42**, 1589; (b) Z. Li, W. Wu, G. Qiu, G. Yu, C. Ye, Y. Liu, J. Qin and Z. Li, *J. Polym. Sci., Part A: Polym. Chem.*, 2011, **49**, 1977; (c) W. Wu, Y. Fu, C. Wang, C. Ye, J. Qin and Z. Li, *Chem.-Asian J.*, 2011, **6**, 2787; (d) W. Wu, C. Ye, G. Yu, Y. Liu, J. Qin and Z. Li, *Chem.-Eur. J.*, 2012, **18**, 4426.
- C. R. Moylan, R. D. Miller, R. J. Twieg, V. Y. Lee, I. H. McComb, S. Ermer, S. M. Lovejoy and D. S. Leung, *Proc. SPIE-Int. Soc. Opt. Eng.*, 1995, **2527**, 150.
- P. A. Sullivan, H. Rommel, Y. Liao, B. C. Olbricht, A. J. P. Akelaitis, K. A. Firestone, J.-W. Kang, J. Luo, J. A. Davies, D. H. Choi, B. E. Eichinger, P. J. Reid, A. Chen, A. K.-Y. Jen, B. H. Robinson and L. R. Dalton, *J. Am. Chem. Soc.*, 2007, **129**, 7523.
- M. Kauranen, T. Verbiest, C. Boutton, M. N. Teeren, K. Clays, A. J. Schouten, R. J. M. Nolte and A. Persoons, *Science*, 1995, **270**, 966.
- (a) Q. Li, Z. Li, C. Ye and J. Qin, *J. Phys. Chem. B*, 2008, **112**, 4928; (b) Z. Li, C. Huang, J. Hua, J. Qin, Z. Yang and C. Ye, *Macromolecules*, 2004, **37**, 371; (c) Z. Li, J. Qin, A. Qin and C. Ye, *Polymer*, 2005, **46**, 363; (d) Z. Li, W. Gong, J. Qin, Z. Yang and C. Ye, *Polymer*, 2005, **46**, 4971.
- (a) Z. Li, J. Hua, Q. Li, C. Huang, A. Qin, C. Ye and J. Qin, *Polymer*, 2005, **46**, 11940; (b) Q. Li, G. Yu, J. Huang, H. Liu, Z. Li, C. Ye, Y. Liu and J. Qin, *Macromol. Rapid Commun.*, 2008, **29**, 798; (c) Z. Li, W. Wu, C. Ye, J. Qin and Z. Li, *Polym. Chem.*, 2010, **1**, 78; (d) Z. Li, J. Qin, S. Li, C. Ye, J. Luo and Y. Cao, *Macromolecules*, 2002, **35**, 9232.